Publishing House
AKAPIT

COMPUTER METHODS IN MATERIALS SCIENCE

Informatyka w Technologii Materiałów

Vol. 13, 2013, No. 1

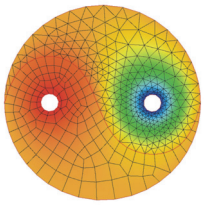

THERMO-MECHANICAL ANALYSIS OF THE POWER TURBINE CASING AT THE RUNNING CONDITIONS

PAWEŁ WOJNAROWSKI[1]*, ANDRZEJ KUŹNIAR[2], STANISŁAW KIEŁBASA[2], LECHOSŁAW TRĘBACZ[1], DANUTA SZELIGA[1], MACIEJ PIETRZYK[1], JACEK ROŃDA[1]

[1] AGH University of Science and Technology, al. Mickiewicza 30, 30-059 Kraków, Poland
[2] WSK "PZL - Rzeszów" S.A., ul. Hetmańska 120, 35-078 Rzeszów, Poland
**Corresponding author: pwojnaro@agh.edu.pl*

Abstract

The paper is the result of the cooperation between WSK Rzeszów company and the AGH within SPAW project. In the paper thermo-mechanical analysis of the power turbine casing for a PZL-10W engine at the running conditions was considered. The goal of the work was evaluation of possibility of prediction of the thermal fatigue in the casing using numerical calculations carried out with commercial software Morfeo, based on the finite element method combined with the material fatigue models. Conventional fatigue models presented in the literature, dedicated to low cycle material fatigue, were implemented as the external procedures to Morfeo, compatible with the interface output data set format. Thermomechanical parameters calculated by the FE program are an input for the fatigue model. The results of the calculations were compared to the results observed in the real casing at the running conditions. The quantitative agreement was approved.

Key words: thermo-mechanical analysis, thermal fatigue, power turbine casing, numerical modeling

1. INTRODUCTION

Structures that are subject to high service temperatures, where creep (and possibly creep-fatigue) is significant, need well defined material behavior. Therefore, the lifetime of these structures requires assessment for all integral structural components. The power turbine casing for airplane engine was investigated in the present work. This is a thin-section generic spoke structure and it is a subject to long cycle thermal cycles during exploitation. High temperature methodologies were applied in this paper to this complicated geometry, including a weld with differing material properties.

Life assessment of welded thin-section structures is particularly complex. It is due to residual stresses, distortions and material microstructural changes caused by the welding process. Since sharp fillet radii result in high stress concentrations at the weld bead and parent interface, the weld bead geometry must be considered. Due to these factors, the weld has a direct effect on the creep and fatigue life (Tanner et al., 2009).

2. POWER TURBINE CASING

Although it has several disadvantages, welding (as opposed to casting) reduces the cost of large thin-section structural components and can eliminate the need to transport full size cast components from the supplier to the manufacturer, which is also more cost efficient and better for the environment (Tanner et al., 2009). As such, welding is an integral manufacturing procedure for many components, some of which could not be produced without its application.

ISSN 1641-8581

The power turbine casing for a PZL-10W engine was investigated in the present work. A simplified geometrical model of this turbine was created. The simplification of the geometry consisted in the removal of unnecessary components and geometric features such as holes, cutouts, chamfers and fillets, all of which had no significant effect on the thermal stress calculations. Figure 1 shows the simplified geometry of the turbine casing and a ¼ part of the model used for numerical simulations.

Table 1. *The properties for 321 Steel and Inconel 625.*

	321Steel	IN625
Young modulus, GPa	193	204.8
Poisson ratio	0.3	0.3
Density, kg/m^3	8000	8440
Thermal conductivity, W/mK	16.78	9.8
Specific heat, J/kgK	500	410
Coefficient of thermal expansion, 10^{-6} cm/cmK	16.92	13.02

Fig. 1. *A simplified model of the geometry of the power turbine casing for a PZL-10W engine.*

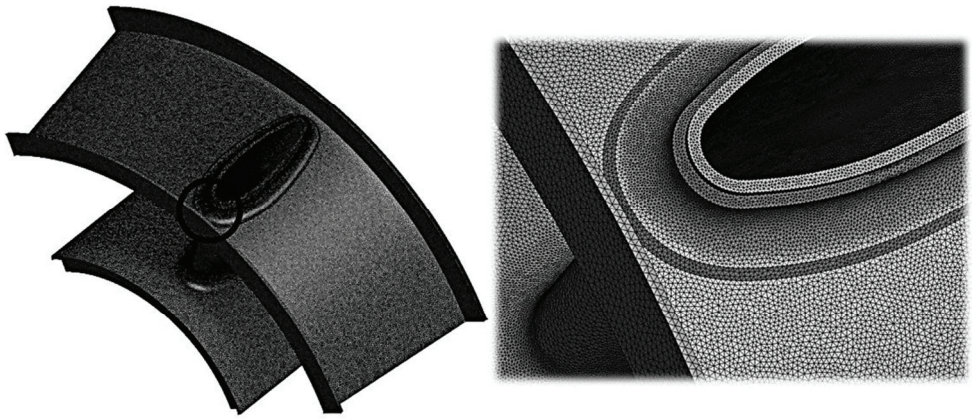

Fig. 2. *Finite element mesh of the tetra-type elements for ¼ part of the turbine casing.*

The main material used throughout this study was sheet metal made of Inconel 625 (IN625), a precipitation-hardenable, niobium-modified, nickel-base super alloy. Since this alloy exhibits good strength, excellent resistance to oxidation at high temperatures and favorable weldability, it is extensively used in the aerospace, petrochemical, and nuclear industries. The power turbine casing is composed of two materials. Besides Inconel 625, which was used for inner and outer rings and for the turbine deflectors and welds, 321 steel of which the clamping rings to other engine units were made was considered, as well. Table 1 shows the properties of both investigated materials.

3. NUMERICAL MODEL

3.1. Finite element model

Numerical calculations were performed by the finite element method (FEM) using a Morfeo application developed by Cenareo. The finite element mesh was developed in a Gmsh application coded by Geuzaine et al. (2009). This application allows proper definition of the surface, which is required in the Morfeo software. The mesh consisted of about 1 000 000 of tetra-type elements, and it was refined in areas of the modeled welds. However, due to the presence of thin and long rings, the mesh refinement along the thickness included 2-3 elements, which might cause numerical errors. Figure 2 shows the geometrical model with the applied finite element mesh.

The Fourier thermal boundary conditions were assumed on all surfaces. Various heat exchange coefficients for various cooling conditions were introduced, see table 2. Values of these coefficients are based on an inverse analysis performed by Kuźniar et al. (2011). The mechanical and thermal boundary conditions are shown in table 2, as well. These conditions compose radial and axial forces acting on the turbine casing. Figure 3 shows the boundary conditions used for a model of the turbine casing with well defined surfaces.

Table 2. *List of the mechanical boundary conditions with respect to the specific areas defined in a model mesh and in the input file to Morfeo application.*

Boundary Conditions	Surface number	Value
Radial Force	2	$F = 2400$ N,
Axial Force	3	$F = 1170$ N,
Convection from the air	5, 11	50 W/m^{2}K
Convection from the flue gas	6, 12	200 W/m^{2}K
Convection from the liquid	2, 21, 22	250 W/m^{2}K
Emissivity for Inconel and Steel	5, 6, 14, 15, 18, 19, 21, 40, 2, 3, 4, 7, 11, 12, 13, 16, 17, 20, 22, 23	0.5
Symmetry in Y	8	$\Delta X = 0$
Symmetry in X	9	$\Delta Y = 0$
Fixed point P1	28	$\Delta X = 0, \Delta Z = 0$
Fixed point P2	29	$\Delta Y = 0, \Delta Z = 0$

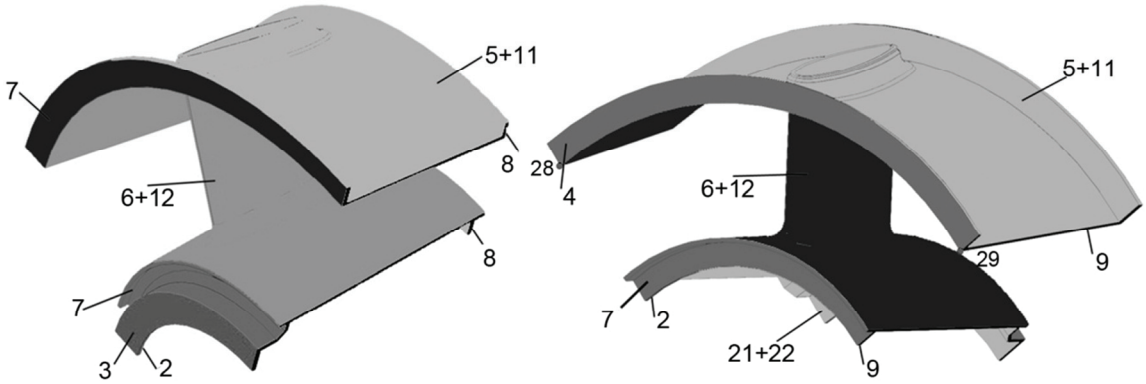

Fig. 3. *The geometrical model with selected defined surfaces and the boundary conditions.*

3.2. Fatigue analysis

Fatigue analysis was perform with the models dedicated to low cycle fatigue (LCF) presented below. The Smith, Watson and Topper (SWT) model was considered (Smith et al., 1970). The number of cycles to failure (N_{fSWT}) in that model is calculated as:

$$N_{fSWT} = \sqrt[\beta_1]{\frac{C_1\left(1-\frac{\sigma_{\max}}{\sigma_y}\right)}{\Delta\sigma}} \tag{1}$$

where: $\sigma_{\max}$ – maximum principal stress, σ_y – yield stress, $\Delta\sigma$ – principal stress amplitude, β_1, C_1 – empirical coefficients ($\beta_1 = 0.06$, $C_1 = 1573.19$).

The next model was proposed by Basquin and it is derived from Coffin model (Afazov, 2009; Basquin, 1910; Wang et al., 2008). In this model the number of cycles to failure is:

$$N_{fB} = \sqrt[\beta_2]{\frac{C_2}{\Delta\sigma}} \tag{2}$$

where: β_2, C_2 – empirical coefficients ($\beta_2 = 0.097$, $C_2 = 1948.71$).

These SWT and Basquin parameters correlates well with cycles to failure using the test data obtained from literature for SWT (Susmel et al., 2011) and Basquin (Afazov, 2009).

4. RESULTS AND DISCUSSION

Numerical calculations consisted in simulation of a single thermal cycle of the engine running. This cycle was divided into four calculation steps:

1. heating – engine start (t = 60 s) – temperature increase,
2. heating – transient to take off (t = 120 s) – temperature increase,
3. heating – take off (t = 220 s) – temperature stabilization,
4. cooling – deceleration to idle range (t = 400 s) – temperature decrease – temperature stabilization – engine stop.

The times of individual steps were calculated from the temperature distribution diagram plotted during the engine operation, shown in figure 4 in bold. The numerical calculations made in a single step included the non-linear thermal process and mechanical process.

results vary slightly in terms of cooling, which is due to a larger calculation step adopted. The temperature obtained in the experimental studies was 546°C and 475°C for the outer and inner ring, respectively. The temperature obtained in the numerical simulation was 545°C and 478°C, respectively.

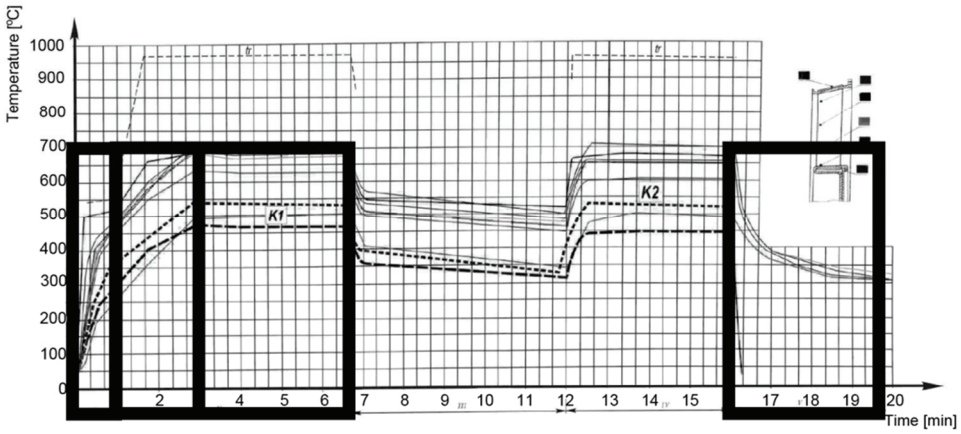

Fig. 4. *Monitored thermal cycle with marked areas chosen for numerical calculations as various stages of the engine operation.*

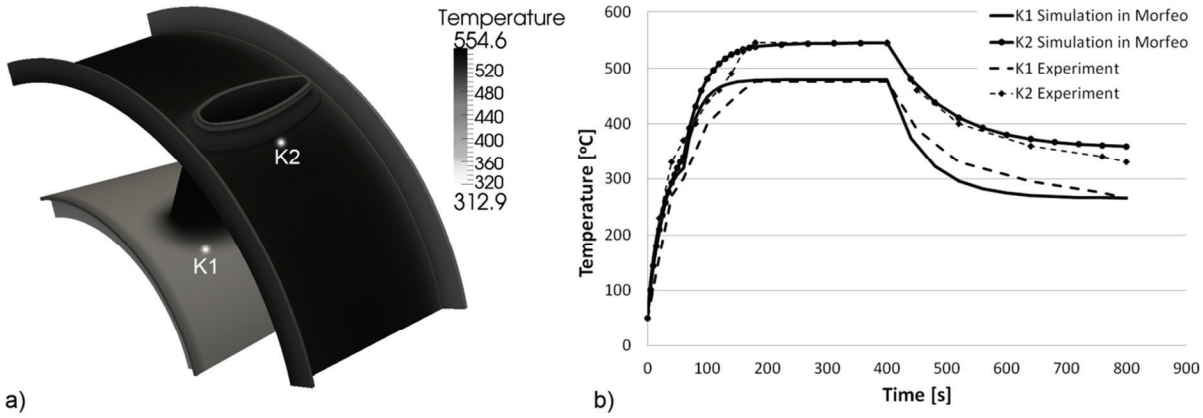

Fig. 5. *a) Temperature distribution in the turbine casing and b) in selected nodes on the bottom (K1) and top (K2) surface [°C].*

4.1. Thermal stresses

The main aim of the first step of the numerical calculations was to determine the thermal stresses occurring in the power turbine casing. The calculated values of these stresses were used in further part of the study to determine the number of fatigue cycles during operation of the power turbine casing for a PZL-10W engine. Figures 5a and 5b show a comparison of the measured temperature distribution in an inner and outer ring of the casing with that obtained by the numerical simulation performed in a Morfeo application. The experiments were carried out at the WSK Rzeszów. The results of simulations are consistent with the experimental results. The

The results of numerical calculations for a single thermal cycle of the engine running are presented in figure 6. Figure 6a shows Distributions of the reduced stress according to Mises hypothesis, the average stress, the principal stress amplitude are presented respectively in figures 6 a, b and c. Distribution of the displacements, the thermal strains and the effective strains are presented respectively in figures 6 d, e and f. All these results were obtained for the maximum temperature recorded during the entire thermal cycle.

The highest stress concentrations were observed in the outer ring at the point of attachment, in the upper bracket (weld) and in the bends of the bottom weld. The maximum observed value of stress is

closed to the yield strength of the turbine material (450 000 kPa). When this value is exceeded, the material will transform into plastic state with the consequent loss of strength and potential cracks.

sults of numerical calculations for number of cycles fatigue for SWT and Basquin models are presented in figure 7.

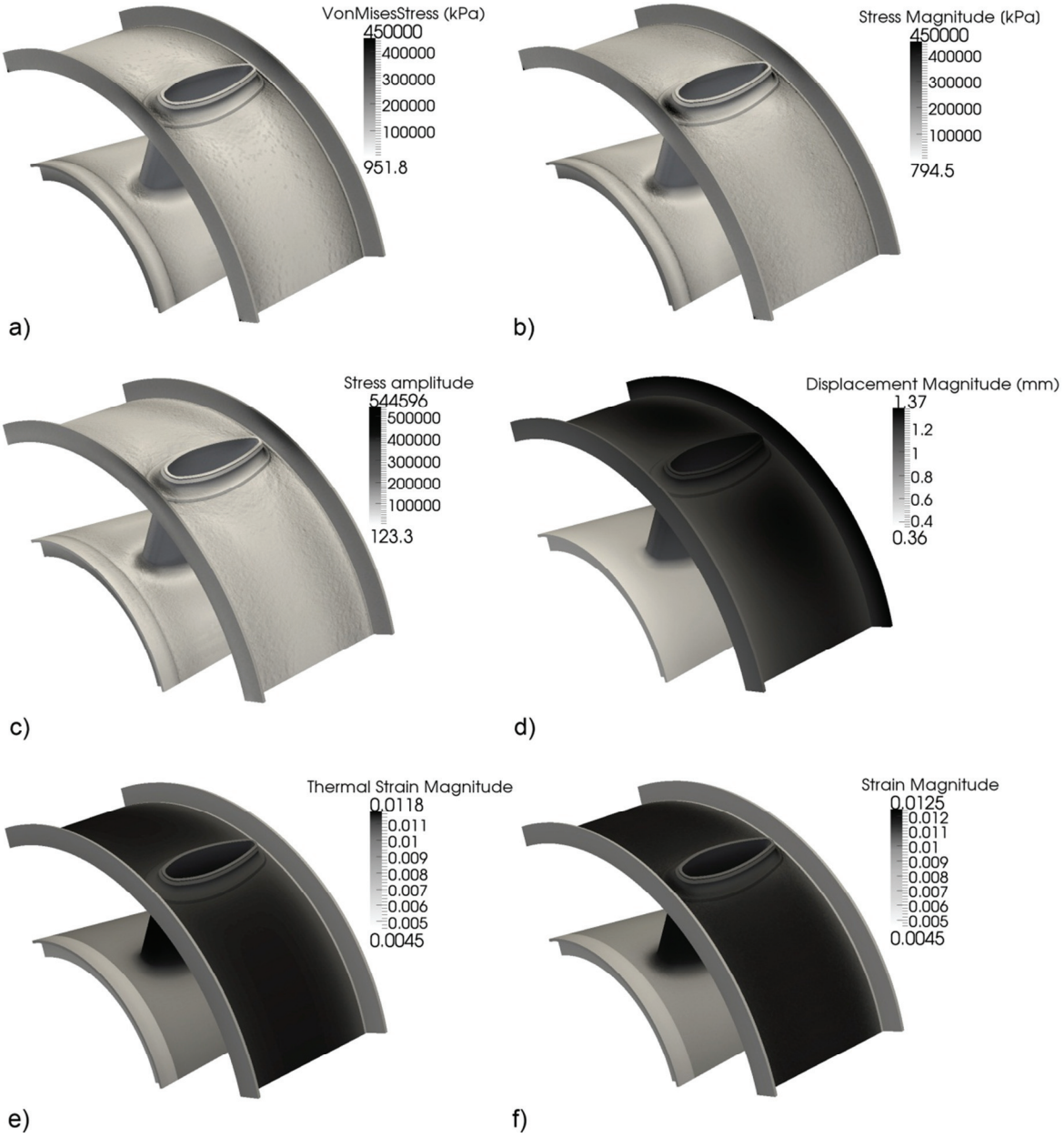

Fig. 6. *Distribution of: a) von Mises stress (effective stress), kPa, b) average stress, kPa, c) principal stress amplitude, kPa, d) displacement, mm, e) thermal strain, f) effective strain.*

4.2. Number of cycles to failure

The results obtained in the first part of simulations allowed calculations of the number of fatigue cycles resulting in the damage of the material. Models of SWT and Basquin were used. The results are shown for the two different fatigue criteria selected from the literature. To calculate the number of fatigue cycles, specially implemented XML libraries serving ParaView application to display the results obtained in Morfeo application were used. The re-

The analysis of the SWT and Basquin models proved that the casing is the most predictive to failure in the place where there are welded parts, deflector with inner ring and the upper bracket welded to the deflector and outer ring (figures 7, dark grey color). In those points the number of the cycles to material failure was the lowest. Comparing to distribution of the maximal stress amplitude it is noticed that there are the same points as for failure criteria. The number of the cycles to material failure is about 10^5.

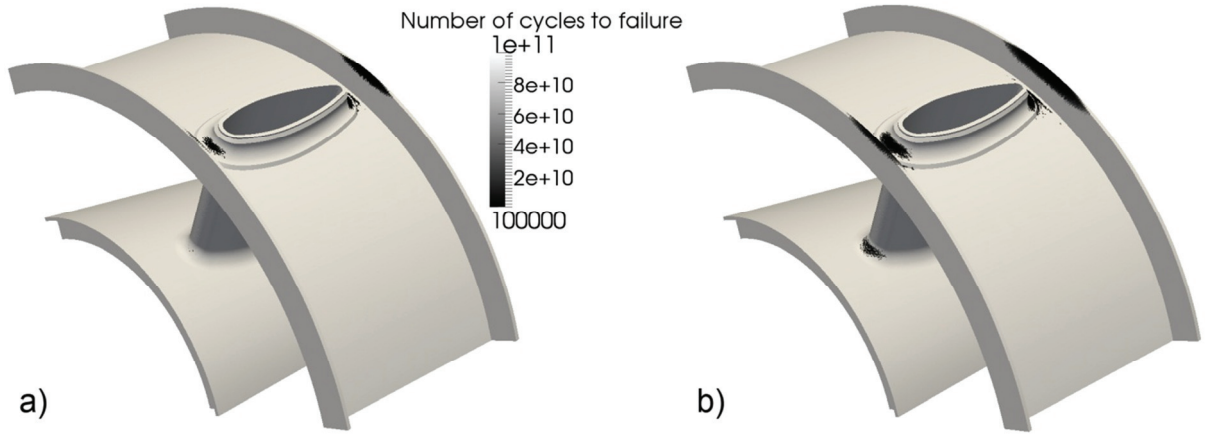

Fig. 7. *Number of cycles fatigue for a) SWT and b) Basquin models.*

5. CONCLUSIONS

Creep and high temperature fatigue properties of the welded IN625 are decreased comparing to the solid material (Tanner et al., 2009). The predicted high temperature fatigue properties of the welded IN625 material have an effect on the high temperature fatigue life of the whole power turbine casing examined here. The predicted failure location was affected by the weld and upper brackets welded to outer ring and deflector. Failure occurred in the regions of greatest stress, namely in the outer ring at the point of attachment, in the upper bracket (weld) and in the bends of the bottom weld. The maximum amplitude of stresses corresponded to the minimum thermal cycles to destruction of material.

Acknowledgements. The work performed within the research project of NCBiR – SPAW, no. ZPB/33/63903/IT2/10 - 2010-06-01.

REFERENCES

Afazov, S., 2009, *Simulation of manufacturing processes and manufacturing chains using finite element techniques*, PhD thesis, University of Nottingham, UK, 2009.

Basquin, O.H., 1910, The exponential law of endurance test, *Proc. ASTM 10*, 625-630.

Geuzaine, C., Remacle, J.F., 2009, Gmsh: a three-dimensional finite element mesh generator with built-in pre- and post-processing facilities, *International Journal for Numerical Methods in Engineering*, 79, 1309-1331.

Kuźniar, A., Rygiel, P., Dudek, S., Gnot, A., Gancarczyk, T., Perzyński, K., 2011, Numerical model of a TIG welding process for the aviation industry, including analysis of the heat transfer, *Computer Methods in Materials Science*, 11, 173-178.

Smith, K.N., Watson, P., Topper, T.H., 1970, A stress-strain function for the fatigue of metals *Journals of Materials*, 5, 767-778.

Susmel, L., Atzori, B., Meneghetti, G., Taylor, D., 2011, Notch and mean stress effect in fatigue as phenomena of elasto-plastic inherent multiaxiality, *Engineering Fracture Mechanics*, 78, 1628-1643.

Tanner, D.W.J., Becker, A.A., Hyde, T.H., 2009, High temperature life prediction of a welded IN718 component, *Journal of Physics*: Conference Series 181, 1-8.

Wang, Q.J., Xua, C.Z., Zheng, M.S., Zhua, J.W., Dub, Z.Z., 2008, Fatigue crack initiation life prediction of ultra-fine grain chromium–bronze prepared by equal-channel angular pressing, *Materials Science and Engineering A*, 496, 434-438.

ANALIZA TERMO-MECHANICZNA OBUDOWY TURBINY NAPĘDOWEJ SILNIKA ODRZUTOWEGO W WARUNKACH EKSPLOATACJI

Streszczenie

Artykuł jest wynikiem współpracy pomiędzy Akademią Górniczo-Hutniczą w Krakowie a zakładem WSK Rzeszów w ramach projektu SPAW. W pracy przeprowadzono analizę termomechaniczną obudowy turbiny napędowej silnika odrzutowego PZL-10W w warunkach jego eksploatacji. Celem pracy była ocena, czy możliwe jest przewidywanie zmęczenia cieplnego materiału obudowy na podstawie obliczeń numerycznych z wykorzystaniem komercyjnego programu Morfeo, opartego na metodzie elementów skończonych, i opracowanych dotychczas modeli zmęczenia niskocyklowego. Model zmęczenia zaimplementowano jako zewnętrzne procedury, zgodne z formatem danych wynikowych programu Morfeo. Wyniki przeprowadzonej w Morfeo analizy termo-mechanicznej były wykorzystane do obliczeń zmęczeniowych. Liczbę cykli potrzebną do zniszczenia materiału dla poszczególnych kryteriów porównano z miejscami zniszczenia materiału rzeczywistych obudów. Wyniki te są zadowalające pod względem jakościowym.

Received: September 20, 2012
Received in a revised form: November 4, 2012
Accepted: November 21, 2012